Two-dimensional Coulomb solid with interaction anisotropy

Cláudio José DaSilva and José Pedro Rino
Departamento de Física, Universidade Federal de São Carlos, 13.565-905 São Carlos, SP, Brazil

Pablo F. Damasceno
Departamento de Física, Universidade Federal de São Carlos, 13.565-905 São Carlos, SP, Brazil
and Applied Physics Department, The University of Michigan, Ann Arbor, Michigan 48109-1040, USA

E. Ya. Sherman
Departamento de Química Física, Universidad del País Vasco–Euskal Herriko Unibertsitatea, 48080 Bilbao, Spain
and IKERBASQUE Basque Foundation for Science, Alameda Urquijo 36-5, 48011 Bilbao, Bizkaia, Spain
(Received 8 March 2010; published 28 April 2010)

Low-dimensional systems of interacting particles demonstrate a variety of fascinating macroscopic properties. Experimentally investigated examples include two-dimensional electron systems in semiconductors structures and Abrikosov vortex lattices in superconductors; these systems share notable features in common, such as low-symmetry host crystal interactions. These interactions can be described in terms of a general statistical model: as systems driven by Coulombic forces and anisotropic bond energy. Through molecular-dynamics simulation we find that the expected hexagonal order disappears even for a weak tetragonal anisotropy, giving rise to a tetragonal structure with a finite-length ordering allowing for determination of the critical anisotropy parameter for the phase transition.

DOI: 10.1103/PhysRevB.81.153307 PACS number(s): 73.20.Qt, 02.70.Ns

Low-dimensional ensembles of interacting particles demonstrate a variety of interesting phases with various types of ordering. One of the most intriguing macroscopic orderings is Wigner crystallization which is based on Coulomb repulsion and originally proposed for electrons in metals.[1] Studies of macroscopic ensembles of electrons demonstrated that this phase can more easily be achieved in two-dimensional (2D) rather than in three-dimensional systems. The first experimental proof was given for electrons levitating over surface of liquid helium in regime of low concentration, where electron motion is classical.[2]

A much broader class of 2D electron systems and experimentally achievable temperature and concentration regimes is presented by carriers in artificial semiconductor structures such as quantum wells and heterojunctions. A result of a balance between electron-electron interaction and quantum kinetic energy of electrons, a 2D Wigner crystal can be stabilized by an external magnetic field perpendicular to the structure.[3] Here, the presence of host lattice strongly influences properties of electron phases, making the understanding of phase diagram a problem of fundamental interest.[4–7] Since different phases of 2D electron ensembles are expected to have energies different within only 0.01 of their values,[5] the effect of coupling to the host lattice can be crucial. Coupling to the host brings about at least two new sets of features in the physics of electron systems. One new set is the effect of a static disorder: the imperfections in the environment, always present there, can drastically affect the electron structure. In the simplest case, a static random potential $U(x,y)$ is coupled to local electron density $n_s(x,y)$ as $U(x,y)n_s(x,y)$. A competition between Coulomb forces and disorder produces elastic and inelastic deformations, pins the electron solid, and leads to a interesting collective phenomena, including the system creeping by an external electric field.[8,9]

The other set of new properties is related to interaction between electrons and excitations in the host lattice. These features become very attractive to study since structures with a very weak disorder can be produced. To provide an example, a magnetic field perpendicular to the structure causes stripes with a modulated electron density pinned with respect to the host lattice.[10] This behavior was experimentally observed in an anisotropic 2D electron-gas conductivity.[11] The system has a metastable collective state and shows a relaxation at long time scales toward equilibrium. These effects can be attributed to anisotropic contributions to electron-electron interaction induced by a coupling to the host lattice of tetragonal symmetry, which can occur through acoustic-phonon exchange.[12,13] Host-induced interactions, not directly related to density, but lowering the system symmetry, are weak and long range and can be crucial for the system behavior on macroscopic scale, as will be shown below. Perhaps, the first effect of coupling of a monolayer of interacting particles with the host lattice was considered for Ar on graphite,[14,15] where such host lattice forms a periodic potential for Ar adatoms. Other interesting examples of collective interactions to the host system are polaronic effects[16,17] and stripe phases in high-temperature superconductors. The systems of our interest are, however, qualitatively different: here the host lattice creates an additional symmetry-induced particle-particle interaction rather than try to locate particles in the minima of lattice-produced potential.

The interaction between electrons can be understood from Fig. 1. To illustrate the appearance of the additional term in the interaction, we consider phonon-mediated electron-electron scattering matrix elements $M_{ee}^{ph}(\mathbf{k}_1,\mathbf{k}_2,\mathbf{q})$ [Fig. 1(a)] in the crystal structure with tetragonal symmetry. Here electron momenta $\mathbf{k}_1,\mathbf{k}_2$ are in the structure plane while phonon momentum $\mathbf{q}$ can has an arbitrary direction. The Fourier

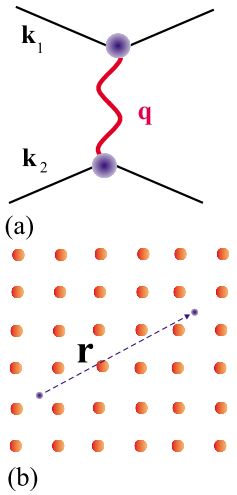

FIG. 1. (Color online) (a) Matrix element for the phonon exchange $M_{ee}^{ph}(\mathbf{k}_1,\mathbf{k}_2,\mathbf{q})$. (b) Host lattice with tetragonal symmetry. Large circles stand for the host lattice and small ones represent electrons.

transform of the matrix element yields the additional phonon-mediated potential in the form,[12,13]

$$U(r) = \frac{e^2}{\varkappa r}(1 + a\cos 4\phi), \tag{1}$$

where r is the distance between electrons, $\varkappa$ is the dielectric constant, and ϕ is the angle between one of the plane axes and $\mathbf{r}$ [Fig. 1(b)]. The coupling constant a determined by the strength of electron coupling to acoustic phonons in the matrix element in Fig. 1(a) will be considered here as a small phenomenological parameter.

Electrons in semiconductor structures is not the only example of possible Wigner crystallization. Other interacting systems, even those not formed by real particles, can show a similar ordering and, as a result, similar effects of coupling to the host lattice.[18] A neat example is the Abrikosov vortex lattice in type-II superconductors.[19] The interaction between vortices is repulsive and, at sufficiently high concentration they form a 2D periodic structure. As in 2D electron systems, various phases of vortex structures have similar energies, different in less than 1% of values. Therefore, the phase diagram can be sensitive to external perturbations, including symmetry lifting. For tetragonal crystals it was proven by generalization of Ginzburg-Landau equations that the Abrikosov lattice can become tetragonal if anisotropy becomes sufficiently strong.[19–21]

Here we formulate and explore a general statistical mechanics model consisting of a sum of isotropic and relatively weak anisotropic Coulomb interactions, presented by Eq. (1), to study effects of a lower host crystal symmetry on a 2D Wigner crystal. With this model we numerically simulate a classical 2D Wigner crystal embedded in a tetragonal host lattice, formulating it for brevity in terms of electrons. We demonstrate that even being weak, this interaction changes the long-range order leading to formation of a short-range ordered tetragonal structure.

The total potential energy of a system with N electrons of charge e can be written as

$$U = \frac{e^2(1+a)}{2\varkappa}\sum_{i=1}^{N}\sum_{i\neq j}^{N}\left[\frac{1}{r_{ij}} + \frac{8a}{1+a}\left(\frac{x_{ij}^4}{r_{ij}^5} - \frac{x_{ij}^2}{r_{ij}^3}\right)\right], \tag{2}$$

where $x_{ij}=r_{ij}\cos\phi$. It will be shown below that these additional terms, weak compared to the Coulomb energy, lead to strong changes in the properties of Wigner solid.

Our numerical simulations are carried out on basis of Langevin molecular dynamics. The equation of motion for an electron is $m\ddot{\mathbf{r}} = -\nabla U(\mathbf{r}) - bm\dot{\mathbf{r}} + \zeta(t)$, where b is the friction coefficient and the thermal noise arises from random Langevin kicks with $\langle\zeta_i(t)\rangle = 0$ and $\langle\zeta_i(t)\zeta_j(t')\rangle = 2mbk_BT\delta_{ij}\delta(t-t')$. Here m is electron effective mass, k_B is the Boltzmann constant, and T is the temperature. The simulations were performed in a rectangular box with area A for a fixed density of 1.2×10^{10} cm^{-2}. The sides of the simulation cell have a ratio of $\sqrt{3}/2$ to allow $4M^2$ electrons to lie in a perfect triangular lattice without any external perturbation. We use periodic boundary conditions and the electron-electron interactions are treated with the Ewald summation. Throughout this paper, we use $\sqrt{A}$ and $E_0 = e^2/2\sqrt{A}$ as units of length and energy, respectively. We use $\tau = \sqrt{mA/2E_0}$ as unit of time. We have made runs with large systems with $N = 1600$ electrons. We set the dielectric constant $\varkappa = 10$ and $m = 0.1$ of the free-electron mass, which are the typical values for semiconductors structures. The charge neutrality of the system is assured by imposing a contribution of a positive background on the total energy. The equilibrium position of electrons is obtained after a run of 10^5 time steps at zero temperature. Other properties are obtained with an additional 5×10^4 steps. Here, we use the dimensionless time integration step as $\Delta t^* = 1.34\times10^{-3}$. It is also possible to use the typical interelectron spacing r_0 related to the mean electron concentration $n_s \equiv 1/\pi r_0^2$ as unit of length.

We concentrate on defined by the minimum potential-energy hexagonal-tetragonal transition, which occurs when a exceeds a certain critical value a_c. The corresponding structure's evolution is shown in Fig. 2, demonstrating a sharp transition. These results show that already for $a > a_c = 0.042$ the long-range hexagonal order is destroyed, aperiodic structures are observed in a narrow interval of a, and a short-range tetragonal structure is quickly formed.

To study the transition quantitatively we calculate the pair correlation function (Fig. 3),

$$g(r) = \frac{1}{Nn_s}\left\langle\sum_{i=1}^{N}\sum_{j\neq i}^{N}\delta(r - r_{ij})\right\rangle, \tag{3}$$

to characterize the distribution of distances between electrons. For numerical calculation $g(r)$ can be presented as,

$$n_s g(r) = \frac{2\bar{N}(r,\Delta r)}{2\pi r\Delta r N}, \tag{4}$$

where $\bar{N}(r,\Delta r)$ is the total number of electrons located between r and $r+\Delta r$ for all electrons considered as the origin. Another possibility is provided by the function describing the coordination number (Fig. 4),

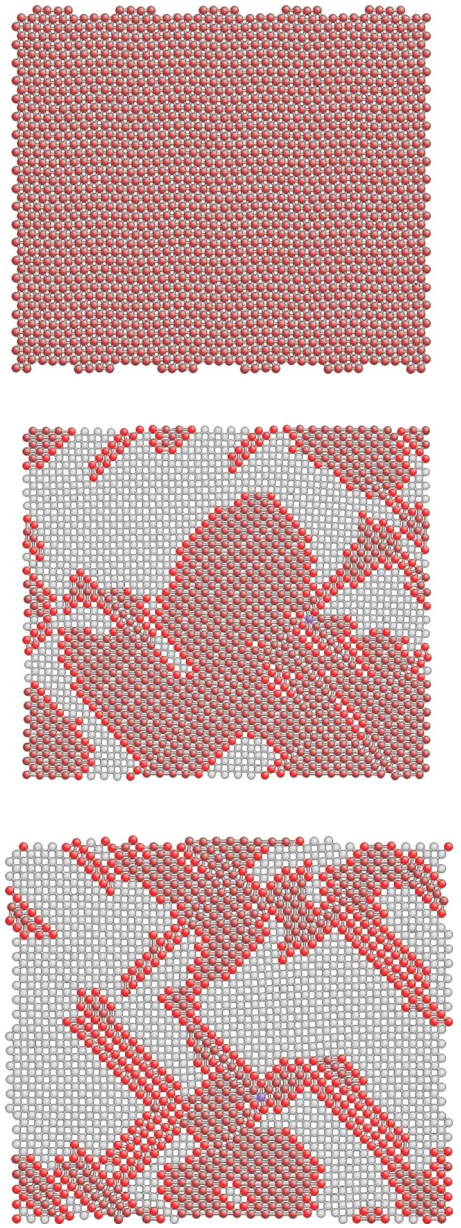

FIG. 2. (Color online) Phases of 2D Coulomb solid at different values of anisotropy: $a=0.41$ (upper panel), $a=0.42$ (middle panel), and $a=0.43$ (lower panel). Dark area—hexagonal structure, light area—tetragonal structure.

$$C(R) = 2\pi n_s \int_0^R rg(r)dr. \tag{5}$$

Figures 3 and 4 confirm that long-range hexagonal order disappears for $a>0.043$ and a tetragonal structure is formed. Another interesting observation is that the formed structure is in fact relatively short range. This can be seen in Figs. 3 and 4 since the weak anisotropic forces compete with the strong isotropic Coulomb interaction. In Fig. 3 the structure peaks remain broad even deeply in new phase. The same observation can be done for Fig. 4, where the plateaus corresponding to the coordination numbers are not flat and show a weak slope with the distance. In addition to the disorder

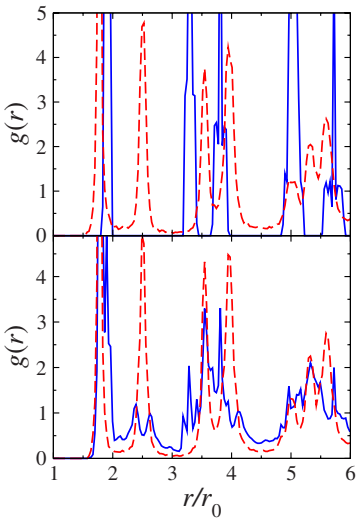

FIG. 3. (Color online) Correlation function $g(r)$. Upper panel: solid line $a=0.041$ and dashed line $a=0.05$. Lower panel: solid line $a=0.042$ and dashed line $a=0.043$. Change in the structure correlation function that occurs between these values of a is clearly seen in the figure.

and transitions related to electron-electron bond length, we have studied orientational disorder related to the distribution of angles between the bonds, and therefore to the crystal symmetry. For this purpose we introduce a local parameter characterizing orientation of the bonds in the vicinity of a given lattice site $\mathbf{R}_0$,

$$\Psi_n(\mathbf{R}_0) = \frac{1}{N_k}\sum_{j=1}^{N_k} \exp[in\Theta_j(\mathbf{R}_0)], \tag{6}$$

where N_k is the local coordination number of the particle at $\mathbf{R}_0$ determined by the Voronoi tessellation and Θ_j is the angle made by a bond between a particle at the $\mathbf{R}$ point and its nearest neighbor with respect to an arbitrary fixed axis. The corresponding correlation function has the form,

$$g_n(\mathbf{r}) = \langle \Psi_n^*(\mathbf{R}_0)\Psi_n(\mathbf{R}_0+\mathbf{r})\rangle. \tag{7}$$

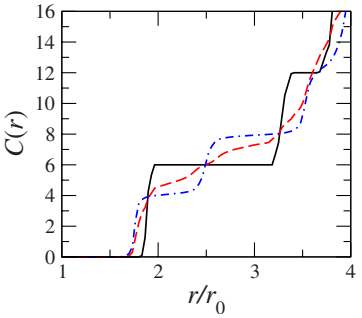

FIG. 4. (Color online) Correlation function $C(R)$ shown the number of neighbors as a function of the distance. Solid line $a=0.041$, dashed line $a=0.042$, dashed-dotted line $a=0.043$. The plateaus in the tetragonal phase at $C(R)=4$ and $C(R)=8$ have a finite slope corresponding to the finite spatial scale of the ordering.

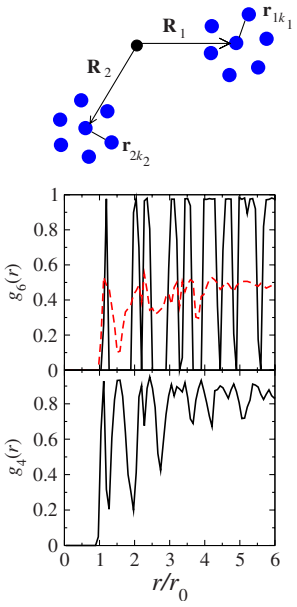

FIG. 5. (Color online) (Upper panel) Illustration for $g_n(\mathbf{r})$ function. (Middle panel) Function $g_6(\mathbf{r})$ characterizing the hexagonal orientational order. Solid line $a=0.041$ and dashed line $a=0.042$. (Lower panel) Function $g_4(\mathbf{r})$ characterizing the tetragonal orientational order for $a=0.043$. The cutoff is taken at $r_{co}=2.15r_0$.

These parameters characterize the bond-direction disorder shown in Fig. 5. The behavior of $g_n(\mathbf{0})$ characterizes the local distribution of the angles between the bonds to neighbors of a given electron. To characterize the hexagonal-tetragonal transition, we consider two parameters, $g_6(\mathbf{r})$ and $g_4(\mathbf{r})$, which show a well-structured behavior in the hexagonal and tetragonal structures, respectively.[22–24] Due to imperfect tetragonal ordering, the parameter $g_4(\mathbf{r})$ depends on cutoff r_{co} performed in the calculation: neighbors at the distances $r > r_{co}$ are not included in Eq. (6).

To conclude, we have investigated a 2D Wigner crystal with anisotropic bond energies: the model for 2D electrons in solids and Abrikosov superconducting vortex lattices. The changes in the crystal structure brought about by the anisotropy are seen in $g(r)$ and angular $g_4(r)$ and $g_6(r)$ correlation functions, characterizing the pair distances and orientational order, respectively. By the Langevin molecular simulation we found a small critical value of anisotropy close to 0.04 showing that even a weak anisotropic contribution in the Coulomb force leads to a transition between long-range ordered hexagonal and short-range ordered tetragonal structures. This value is in a very good agreement with calculations on Abrikosov vortex structure based on solution of Ginzburg-Landau equations,[21] revealing the fact that the physics brought about by the anisotropy in these two systems is common despite different original scales of interaction. Our results can be applied to analysis of various systems where weak anisotropic interactions compete with strong long-range forces.

We thank the financial support provided by the Brazilian agencies: CAPES, CNPq, and FAPESP. E.Y.S. thanks the University of the Basque Country (Grant No. GIU07/40) and the MCI of Spain (Grant No. FIS2009-12773-C02-01).

[1] E. Wigner, Phys. Rev. **46**, 1002 (1934).
[2] Y. Monarkha and K. Kono, *Two-Dimensional Coulomb Liquids and Solids* (Springer, New York, 2004).
[3] E. Y. Andrei, G. Deville, D. C. Glattli, F. I. B. Williams, E. Paris, and B. Etienne, Phys. Rev. Lett. **60**, 2765 (1988).
[4] T. Ando, A. B. Fowler, and F. Stern, Rev. Mod. Phys. **54**, 437 (1982).
[5] L. Bonsall and A. A. Maradudin, Phys. Rev. B **15**, 1959 (1977).
[6] E. Fradkin and S. A. Kivelson, Phys. Rev. B **59**, 8065 (1999).
[7] B. A. Piot, Z. Jiang, C. R. Dean, L. W. Engel, G. Gervais, L. N. Pfeiffer, and K. W. West, Nat. Phys. **4**, 936 (2008).
[8] R. Chitra, T. Giamarchi, and P. Le Doussal, Phys. Rev. Lett. **80**, 3827 (1998); Phys. Rev. B **65**, 035312 (2001).
[9] C. J. da Silva, J. P. Rino, and L. Cândido, Phys. Rev. B **77**, 165407 (2008).
[10] K. B. Cooper, J. P. Eisenstein, L. N. Pfeiffer, and K. W. West, Phys. Rev. Lett. **92**, 026806 (2004).
[11] M. P. Lilly, K. B. Cooper, J. P. Eisenstein, L. N. Pfeiffer, and K. W. West, Phys. Rev. Lett. **82**, 394 (1999).
[12] E. Ya. Sherman, Phys. Rev. B **52**, 1512 (1995); E. I. Rashba and E. Y. Sherman, Sov. Phys. Semicond. **21**, 1185 (1987).
[13] D. V. Fil, J. Phys.: Condens. Matter **13**, 11633 (2001); Physica E **14**, 355 (2002).
[14] J. P. McTague and A. D. Novaco, Phys. Rev. B **19**, 5299 (1979).
[15] Similar problems are now considered for adatoms on graphene: V. V. Cheianov, V. I. Falko, O. Syljuasen, and B. L. Altshuler, Solid State Commun. **149**, 1499 (2009).
[16] G. A. Farias and F. M. Peeters, Phys. Rev. B **55**, 3763 (1997).
[17] G. Rastelli, P. Quémerais, and S. Fratini, Phys. Rev. B **73**, 155103 (2006).
[18] In addition, we mention that a classical ionic Wigner solid physics can be responsible for properties of polyelectrolytes and colloids: B. I. Shklovskii, Phys. Rev. Lett. **82**, 3268 (1999); A. Y. Grosberg, T. T. Nguyen, and B. I. Shklovskii, Rev. Mod. Phys. **74**, 329 (2002); F. M. Peeters and X. Wu, Phys. Rev. A **35**, 3109 (1987).
[19] G. Blatter, M. V. Feigel'man, V. B. Geshkenbein, A. I. Larkin, and V. M. Vinokur, Rev. Mod. Phys. **66**, 1125 (1994).
[20] I. Affleck, M. Franz, and M. H. Sharifzadeh Amin, Phys. Rev. B **55**, R704 (1997).
[21] K. Park and D. A. Huse, Phys. Rev. B **58**, 9427 (1998).
[22] M. C. Cha and H. A. Fertig, Phys. Rev. Lett. **73**, 870 (1994); Phys. Rev. B **50**, 14368 (1994).
[23] S. Z. Lin, B. Zheng, and S. Trimper, Phys. Rev. E **73**, 066106 (2006).
[24] P. S. Branício, J.-P. Rino, and N. Studart, Phys. Rev. B **64**, 193413 (2001).